# Datasheet-based modeling of Li-Ion batteries

Barreras, Jorge Varela; Schaltz, Erik; Andreasen, Søren Juhl; Minko, Tomasz

*Published in:*
Proceedings of the 2012 IEEE Vehicle Power and Propulsion Conference

*DOI (link to publication from Publisher):*
10.1109/VPPC.2012.6422730

*Publication date:*
2012

*Document Version*
Early version, also known as pre-print

# Datasheet-based modeling of Li-Ion batteries

Jorge Varela Barreras*, Erik Schaltz, Søren Juhl Andreasen, Tomasz Minko
Department of Energy Technology, Aalborg University, Aalborg 9220, Denmark
jvb@et.aau.dk*

***Abstract* – Researchers and developers use battery models in order to predict the performance of batteries depending on external and internal conditions, such as temperature, C-rate, Depth-of-Discharge (DoD) or State-of-Health (SoH). Most battery models proposed in the literature require specific laboratory test for parameterization, therefore a great majority do not represent an appropriate and feasible solution. In this paper three easy-to-follow equivalent circuit modeling methods based only on information contained in a commercial Li-Ion cell manufacturer's datasheet are presented and validated at steady state, comparing simulation results and manufacturer's curves. Laboratory results are included in order to demonstrate the accuracy of parameters estimation. Results of each method are presented, compared and discussed for a Kokam SLPB 120216216 53Ah Li-Ion cell.**

**Keywords: battery model, Lithium Ion battery, equivalent circuit model, manufacturer's datasheet.**

## I. INTRODUCTION

It is well known that the performance of batteries varies significantly from the performance of an ideal energy source. In fact batteries are highly non-linear electrochemical systems, governed by a complex mixture of laws of thermodynamics, electrode kinetics and ion transport phenomena. During the last 25 years, numerous mathematical models have been developed by researchers and developers to predict the behavior of batteries, depending on a combination of external and internal conditions [1]:

- Internal: Depth-of-Discharge (DoD), State-of-Health (SoH), impedance, battery design parameters (chemistry, geometry, electrolyte concentration, electrode thickness, etc.) or self-discharge rate.
- External: temperature, C-rate, short-term and long-term history (i.e. cycle life of secondary cells).

The purpose of using battery models can be either [2]:

- To estimate the impact of a preliminary design.
- To estimate the performance of battery already manufactured under specific conditions of interest.

As a rule of thumb it can be stated that more complex models give more exact and accurate results, but require higher computational complexity and higher configuration effort – moreover specific characterization tests require specific (and expensive) laboratory equipment [2-6]. It can also be stated that in some cases simple battery models are the most appropriate and feasible solution, e.g. in early stages of the system design process, in non-focused battery applications or whenever low computational complexity or low configuration effort is a requirement. A brief overview of modeling approaches and applications is given in Table 1 [2-6].

TABLE I

OVERVIEW OF BATTERY MODELING APPROACHES AND APPLICATIONS

| Model approach | Accuracy | Computational Complexity | Configuration Effort | Analytical Insight | Purpose |
|---|---|---|---|---|---|
| Physical | Very High | High | Very High | Low | Battery design and model validation |
| Empirical | Low-Medium | Low | Low | Low | Battery performance estimation |
| Abstract | Low-High | Low-Medium | Low-High | Medium | Battery performance estimation |
| Mixed | High | Medium | Low-Medium | High | Battery performance estimation |

Since most battery models proposed in literature require specific parameters obtained with laboratory equipment like frequency response analyzers, high capacity current and voltage controlled bipolar power sources, oscilloscopes, data acquisition systems, calorimeters, temperature chambers, zero resistance ammeters and even more complex electrochemical equipment for post-mortem analysis, very often they are not an appropriate and feasible solution.

In this paper three easy-to-follow modeling methods based only on information contained in a typical commercial Li-Ion cell manufacturer's datasheet are presented, simulated and validated at steady state, including laboratory results to demonstrate the accuracy of the parameter estimation. It should be emphasized that all the information needed is included in datasheets and no laboratory tests are required to parameterize the models.

All the proposed modeling methods are based on equivalent circuit models (abstract approach) and some could be operated in combination (mixed approach) with thermal (physical) or ageing models (empirical approach). Some of the models take into account C-rate and temperature effects on the Open Circuit Voltage vs. DoD characteristic curve, as well as the DoD dependency on the charge and discharge inner resistances. Short term battery dynamics are not considered (typically represented by RC elements in equivalent circuits), since information required for this task is not found in datasheets. Results for a commercial battery are presented, compared and discussed.

## II. EQUIVALENT CIRCUIT BATTERY MODELS

Equivalent circuit models (ECM) use electrical circuits to simulate the real performance of a certain device. In case of batteries, e.g. a capacitor can be used to model the battery capacity while the effect of temperature or DoD variations can be modeled by variable resistors and controlled voltage sources.

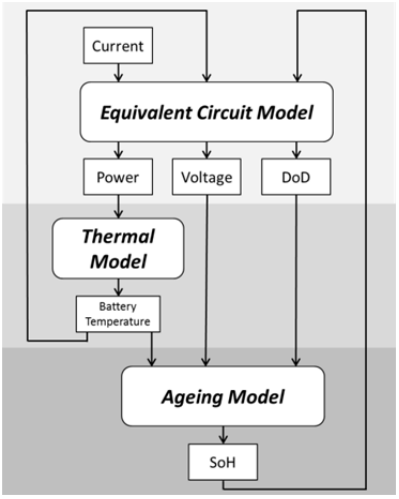


Fig. 1: Overview of typical 3-level model structure.

If the effects of temperature and SoH variations are not considered, simply ECMs are used to estimate the battery behavior. However, if those effects are taken into account thermal and ageing models are integrated in the model (mixed approach) [6].

Such mixed models are typically organized in a three level structure: thermal model use outputs from ECM to predict battery temperature; at the same time ageing model use outputs from thermal and ECM to predict SoH; finally ECM predict voltage (or current), power and DoD according to a certain current (or voltage) operation profile, battery temperature and SoH in a closed loop structure as seen in Fig. 1.

In any case different applications emphasize different modeling requirements, resulting in different choices in model design. For example, the optimal design of an energy storage system connected to the electric grid expects maximizing the battery lifetime and minimizing its self-discharge. Accordingly an ageing model and an ECM that considers self-discharge are needed, but not a thermal model since an accurate temperature control is commonly assumed in these systems.

The three proposed easy-to-follow ECMs based in information from manufacturer's datasheet are presented below for a Kokam SLPB 120216216 - 53Ah Li-Ion cell.

### *A. ECM I - Thevenin Battery Model*

The first approach is the simplest. The equivalent electrical circuit consists on a constant inner resistance $R_{int}$ in series with a DC voltage source $V_{OCV}$ , which represents the open circuit voltage (OCV), as shown in Fig. 2.

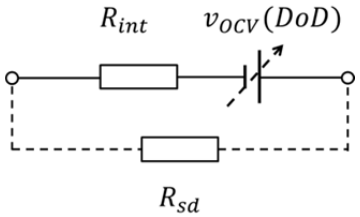


Fig. 2: Thevenin battery model.

In order to include self-discharge effect a resistance $R_{SD}$ could be connected to the battery terminals during rest periods, but no information about self-discharge is usually found on manufacturer's datasheets.

If an ideal DC voltage source is used the effect of DoD variations in OCV are not considered – to consider this effect the DC voltage source can be modeled using (1)

$$v_{OCV}(x) = V_{cha} \cdot \left[1 - \left(\frac{V_{cha}-V_{dis}}{V_{cha}}\right)\left(\frac{\alpha\cdot(1-x)}{1-(1-\alpha)\cdot(1-x)}\right)\right] \quad [V], \qquad (1)$$

where $x$ $[-]$ Ratio of the actual available capacity divided by the total rated capacity.

$V_{cha}$ $[V]$ Full-charge battery voltage.

$V_{dis}$ $[V]$ Full-discharge battery voltage.

$\alpha$ $[-]$ Constant selected according to a certain operating point $(x_1, V_{OCV}(x_1))$, which ensures that the voltage of the battery terminals is equal to $V_{dis}$ when is fully discharged: $V_{OCV}(x = 0) = V_{dis}$.

The previous non-linear equation accounts for the voltage drop at high DOD. In [7] Tremblay et al. proposed another more complex non-linear equation which also accounts for the exponential zone at very low DoD. In this case three operating points are required to parameterize the equation: full-charge, end of exponential zone (when the linear region starts) and end of nominal zone (when the voltage drop begins suddenly).

If more accuracy is pursued, instead of using any of the previous equations, the OCV curve can be estimated directly subtracting the internal resistance voltage drop from the Voltage vs. DoD discharge curve included in datasheets. Fig. 3 shows OCV estimation from Eq. (1) and from the 1C discharge curve for a Kokam 53Ah Li-Ion cell at 23°C considering a constant inner resistance $R_{int} = 1.3\ \text{m}\Omega$ .

It should be noted that this model approach does not consider temperature, SoH variations or Peukert effect. Moreover an identical battery behavior is considered during charge and discharge processes. Therefore its dynamic performance is limited: for instance the accuracy of the simulation will be much lower for high C-rates and high DoD than for C-rates around 1C and DoD over 80%.

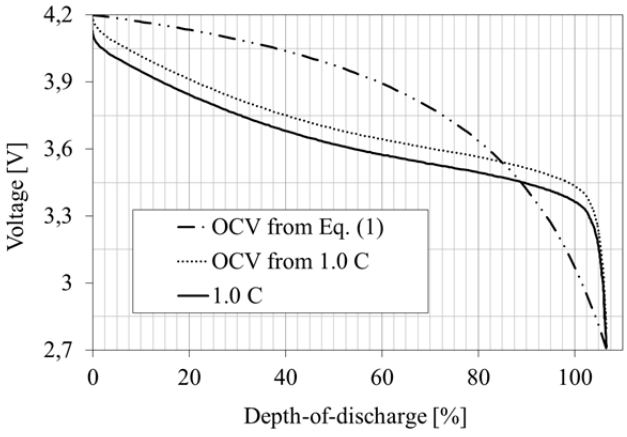


Fig. 3. OCV estimation from Eq. (1) and from 1 C discharge curve.

### B. ECM II – Extended Thevenin battery model 1

The second approach is a more complex model that accounts for C-rate and temperature dependence of the capacity and thermal dependence of the OCV. The ECM from Fig. 4 is an extended version of the previous ECM shown in Fig. 3, but two different inner resistances are considered and a second DC voltage source $\Delta V_{OCV}$ is connected in series – this OCV correction term is used to account for the variation in OCV induced by temperature changes. The two diodes are ideal and have only symbolic meaning, i.e. to be able to switch between the charging and discharging resistances.

Firstly the OCV curve is estimated in the same way proposed for ECM I. Then a modeling procedure based only on datasheet's discharge profiles, similar to the method presented in [10], is followed to calculate the C-rate factor $\alpha$, the temperature factor $\beta$ and the OCV correction term $\Delta V_{OCV}$. Basically a discharge curve from datasheet is chosen as reference, then its x-axis (DoD) distribution and y-axis position (Voltage) is manipulated, using respectively $\alpha$ - $\beta$ factors and $\Delta V_{OCV}$ . The idea is to fit successively this modified curve to each datasheet profile, estimating new values

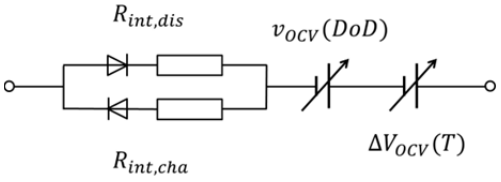


Fig. 4: Extended Thevenin battery model 1.

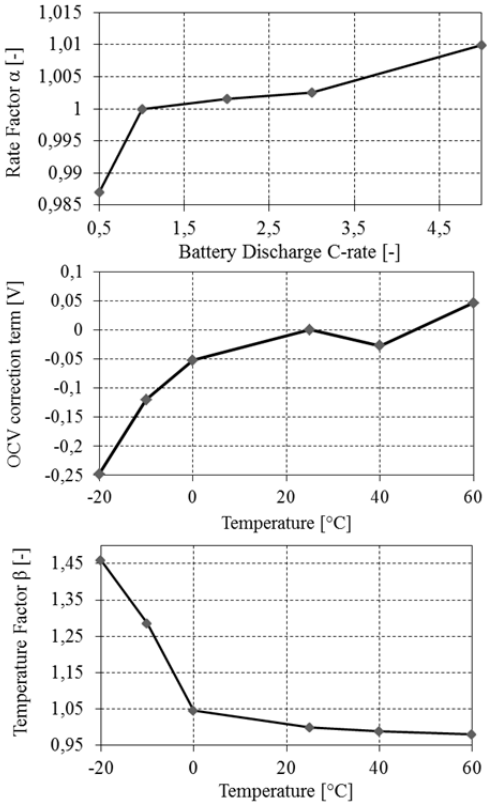


Fig. 5: Calculated rate factor $\alpha$, OCV correction term $\Delta V_{OCV}$ and temperature factor $\beta$.

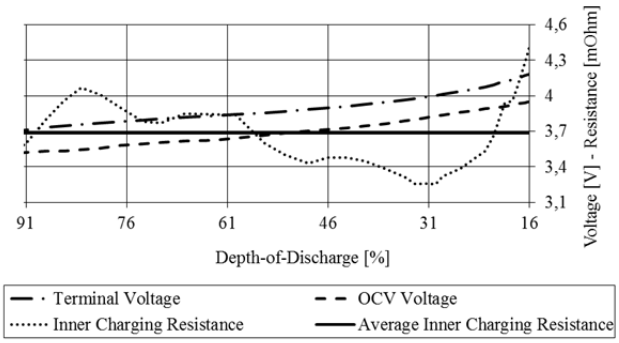


Fig. 6: Estimation of internal charging resistance, $R_{int,cha}$.

of $\alpha$ for each curve of the datasheet with different C-rate, and new values of $\beta$ and $\Delta V_{OCV}$ for each curve of the datasheet with different temperature. Fig. 5 shows results of these calculations for a Kokam 53Ah Li-Ion cell (the reference curve is the 1 C-rate discharge curve and the reference temperature is 25°C).

Using $\alpha$ and $\beta$ factors DoD is calculated as

$$DoD = \frac{100}{Q_{1C} \cdot 3600} \cdot \int_0^t \alpha[i(t)] \cdot \beta[(T(t)] \cdot i\,(t)\,dt + DoD_{t=0}\ [\%]. \quad (2)$$

In this paper, contrary to [10], charge and discharge resistances are different. A new procedure is proposed, using (3) in order to estimate the charging resistance $R_{int,cha}$ from the 1 C-rate CCCV charging curve included in datasheet.

$$R_{int,cha} = (v_{OCV} - v_t)/I_{1C} \qquad [\Omega] \qquad (3)$$

According to this model approach the inner charging resistance $R_{int,cha}$ is considered constant - therefore is decided to estimate its value only from the linear region of the OCV curve (aprox. 91-16% DoD), as shown in Fig. 6, resulting an average inner charging resistance for a Kokam 53Ah Li-Ion cell of $R_{int,cha} = 3{,}69\ \text{m}\Omega$ .

Since temperature effect is considered, the ECM can be operated using an external temperature reference or combined with a thermal model. In [10] a complete set of heat transfer equations (physical approach) is already presented.

### C. ECM III – Extended Thevenin Battery Model 2

The last approach is a new extended version of the last Thevenin model, considering Peukert effect and DoD dependency of charge-discharge inner resistances. The ECM consists on an OCV DC source $V_{OCV}$ and two inner resistances: $R_{int,cha}$ used for charging and $R_{int,dis}$ for discharging. The ECM diagram is shown in Fig. 7.

**Capacity**

Battery capacity dependency on current level phenomena is modeled by manipulating original Peukert equation (empirical approach) [8, 9]

$$Q_{1A} = I_x^k \cdot t_x \qquad [Ah], \qquad (4)$$

where $Q_{1A}[Ah]$ Peukert Capacity.
$I_x$ $[A]$ Discharge current $I = x$ .
$k$ $[-]$ Peukert number.
$t_x$ $[h]$ Discharge time for $I = x$ .

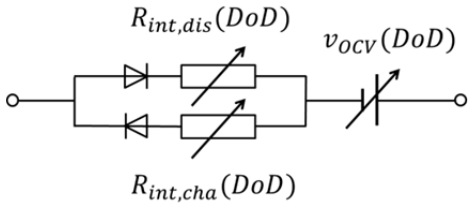


Fig. 7: Extended Thevenin battery model 2.

Original Peukert equation states that the battery capacity (Peukert capacity) is the total capacity in Ah that the battery can deliver at a discharge rate of 1A. In cell specifications capacity is never given in this way, however using the additional term $I_{1C}^{k-1}$ the 1C-rate capacity given in datasheets can be correlated to the Peukert capacity (1A capacity)

$$Q_{1A} = I_{1C}^{k} \cdot t_{1C} = I_{1C}^{k-1} \cdot (I_{1C} \cdot t_{1C}) = I_{1C}^{k-1} \cdot Q_{1C} \ [Ah]. \quad (5)$$

Manipulating (2) and (3) the Peukert number is given by

$$Q_{1A} = I_{1C}^{k} \cdot t_{1C} = I_{x}^{k} \cdot t_{x} \quad [Ah] \quad (6)$$

$$\Rightarrow \quad I_{1C}^{k-1} \cdot (I_{1C} \cdot t_{1C}) = I_{x}^{k-1} \cdot (I_{x} \cdot t_{x}) \quad [Ah] \quad (7)$$

$$\Rightarrow \quad I_{1C}^{k-1} \cdot Q_{1C} = I_{1C}^{k-1} \cdot Q_{x} \quad [Ah] \quad (8)$$

$$\Rightarrow \quad k = \frac{\log(Q_x) - \log(Q_{1C})}{\log(I_{1C}) - \log(I_x)} + 1 \quad [Ah]. \quad (9)$$

So from (7) Peukert number can be derived for any different discharge current included in the datasheet. Known the Peukert number k, capacity fading is included in the equivalent circuit substituting any discharge current by its equivalent current, and the DoD is calculated as

$$I_{x,equiv} = I_{1C} \cdot \left(\frac{I_x}{I_{1C}}\right)^{k} \quad [A] \quad (10)$$

$$\Rightarrow \quad DoD = \frac{100}{Q_{1C} \cdot 3600} \cdot \int_0^t i_{x,equiv}(t)\, dt + DoD_{t=0} \ [\%]. \quad (11)$$

TABLE II

EQUIVALENT DISCHARGE CURRENT FOR KOKAM 53AH LI-ION CELL AT 23°C

| C-rate [-] | 5.0 C | 3.0 C | 2.0 C | 1.0 C | 0.5 C |
|---|---|---|---|---|---|
| I [A] | 268,95 | 159,92 | 106,32 | 53 | 26,11 |

**Inner discharge resistance**

Inner resistance dependencies on DoD variation are derived from the datasheet charge-discharge curves. For two different fractions $x_1$ and $x_2$ of the nominal discharge current $I_{1C}$ the terminal voltage $v_t$ is given by

$$v_t(x_1 \cdot I_{1C}, DoD) = v_{OCV}(DoD) - R_{int,dis}(DoD) \cdot x_1 \cdot I_{1C} \quad [V] \quad (12)$$

$$v_t(x_2 \cdot I_{1C}, DoD) = v_{OCV}(DoD) - R_{int,dis}(DoD) \cdot x_2 \cdot I_{1C} \quad [V]. \quad (13)$$

If it is assumed that the inner discharge resistance $R_{int,dis}$ is independent on the current level, the resistance can be calculated from two data sets, i.e.

$$R_{int,dis}(DoD) = \frac{v_t(x_1 \cdot I_{1C}, DoD)}{(x_2 - x_1) \cdot I_{1C}} - \frac{v_t(x_2 \cdot I_{1C}, DoD)}{(x_2 - x_1) \cdot I_{1C}} \quad [\Omega]. \quad (14)$$

Therefore, for each pair of data sets shown in datasheets the internal resistance is calculated. Since the resistance is considered current independent, the discharge resistance used in the ECM for each DoD value is equal to the average value of this resistance for all the different current fractions included in datasheet CC discharge curves.

**Open Circuit Voltage**

For each current fraction shown in datasheets, the OCV dependency on DoD variations can be estimated as

$$v_{OCV} = v_t + R_{int,dis} \cdot I_{x,equiv} \quad [V]. \quad (15)$$

Applying previous equation to different current fractions included in datasheets, the average OCV vs. DoD characteristic curve is derived.

**Internal Charging Resistance**

The charging resistance $R_{int,cha}$ can be calculated as well from the typical CCCV charging curves included in datasheets using (16)

$$R_{int,cha} = (v_{OCV} - v_t)/I_x \quad [\Omega]. \quad (16)$$

The charge resistance used in the ECM for each DoD value is assumed equal to the average value of this resistance for all the different current fractions included in datasheet CCCV charge curves.

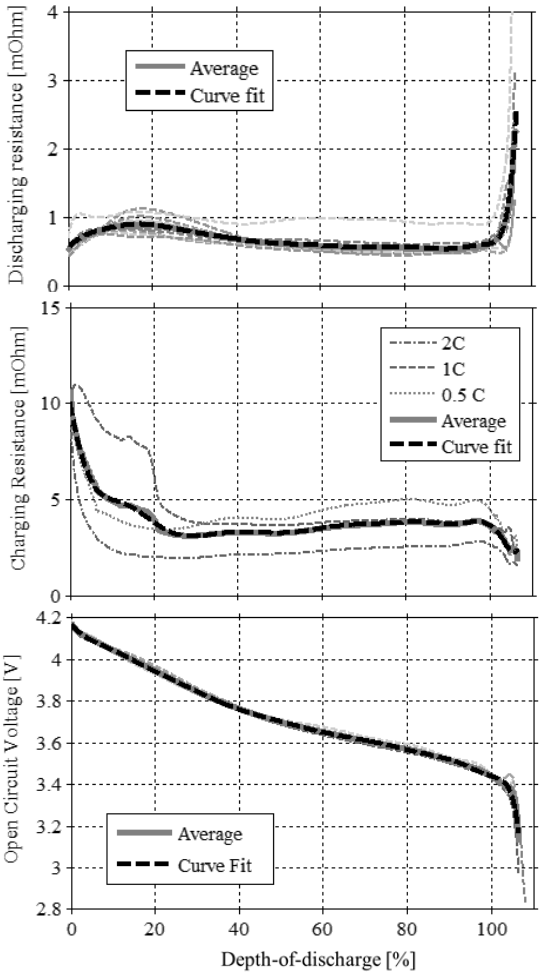


Fig. 8: Estimated inner discharging resistance $R_{int,dis}$ , charging resistance $R_{int,cha}$ and OCV curve.

Figure 8 shows estimation of inner resistances and OCV characteristic for a Kokam 53Ah Li-Ion cell.

## III. Model Validation

The ECMs proposed are validated at steady state, comparing simulation results and datasheet curves for a Kokam SLPB 120216216 - 53Ah Li-Ion cell.

Simulation results are superimposed on typical manufacturer discharge profiles at reference temperature (Fig. 9, 10 and 11). It can be seen that simulation results match well for all ECMs. For ECM III higher accuracy is observed for higher C-rates due to inner resistance variation. For ECM II and III also higher accuracy can be seen for high DoD since Peukert effect is considered.

For the ECM II, since temperature dependencies are taken into account, simulation results are also superimposed on manufacturer temperature characteristics for 1 C-rate (Fig. 12). Simulation results match very well with datasheet, but lower accuracy is expected for higher C-rates.

Due to space constraints, only simulation results are superimposed on datasheet charge profiles for ECM III, since during charging the best performance is obtained for this ECM (Fig. 13). Higher accuracy would be achieved if current dependency is also considered for inner charging resistance.

Finally, in order to validate the method followed for the ECM III, manufacturer charge-discharge characteristics are reproduced in the lab for a real Kokam 53Ah Li-Ion cell. Inner resistances and OCV characteristic estimated from these profiles are compared with battery parameters extracted from 1 C-rate pulsed current tests. In Fig. 14 good match between experimental and estimated results can be observed.

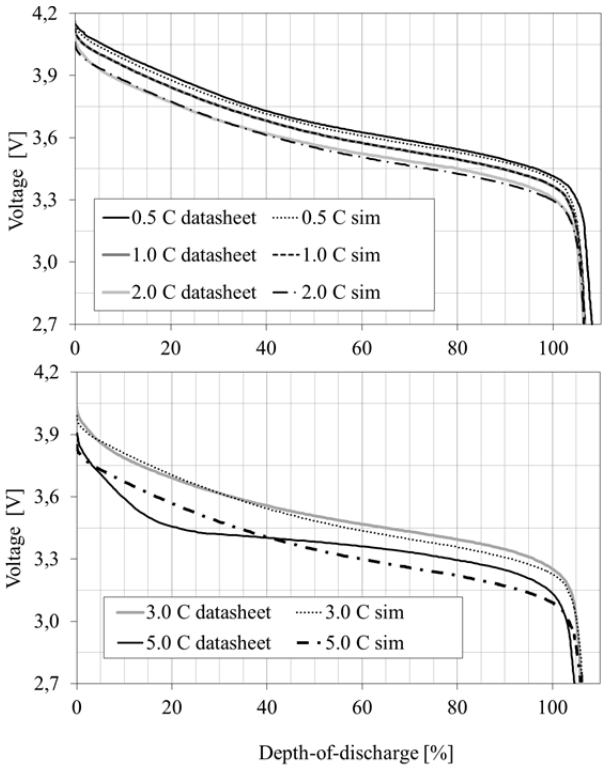


Fig. 9: ECM I simulation results vs. datasheet discharge profiles.

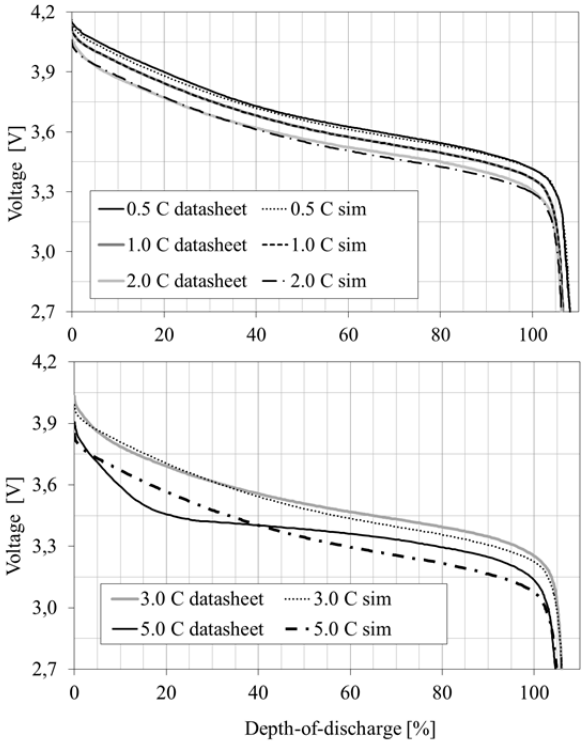


Fig. 10: ECM II simulation results vs. datasheet discharge profiles.

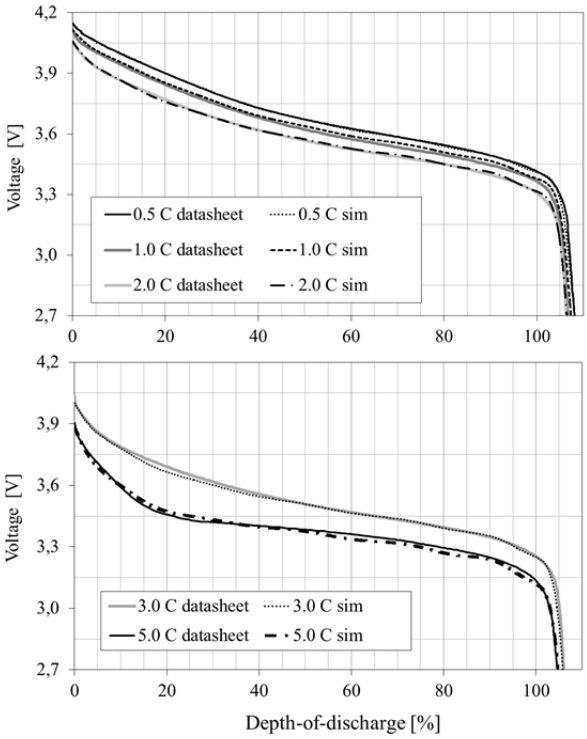


Fig. 11: ECM III simulation results vs. datasheet discharge profiles.

## IV. Conclusions

Three easy-to-follow ECMs that allow an adequate representation of a battery's steady state performance based only on information contained in datasheet are presented and validated in steady state, including models that even take into account DoD dependency on inner charging and discharging

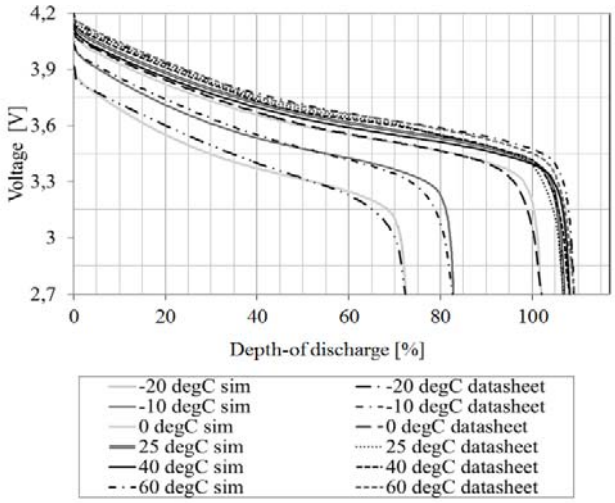


Fig.12: ECM II simulation vs. datasheet temperature characteristics.

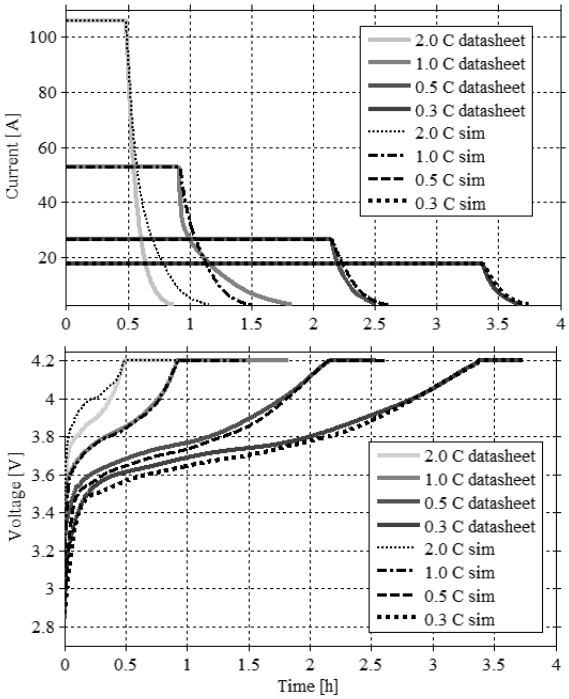


Fig. 13: ECM III simulation results vs. datasheet charge profiles.

resistances and C-rate and temperature effects on the OCV curve. It has also been demonstrated that the values of the inner resistances and the OCV curve estimated using the new method proposed for ECM III are close to experimental values.

It should be noted that the capability of these ECMs to reproduce real battery behavior is limited by the accuracy and veracity of the results shown on manufacturer´s datasheets.

## ACKNOWLEDGMENT

This work, as part of the project "Tomorrow's high-efficiency electric car integrated with the power supply system", is financially supported by The European Regional Development Fund grant number ERDFK-08-0011.

THE EUROPEAN UNION
The European Regional Development Fund
Investing in your future

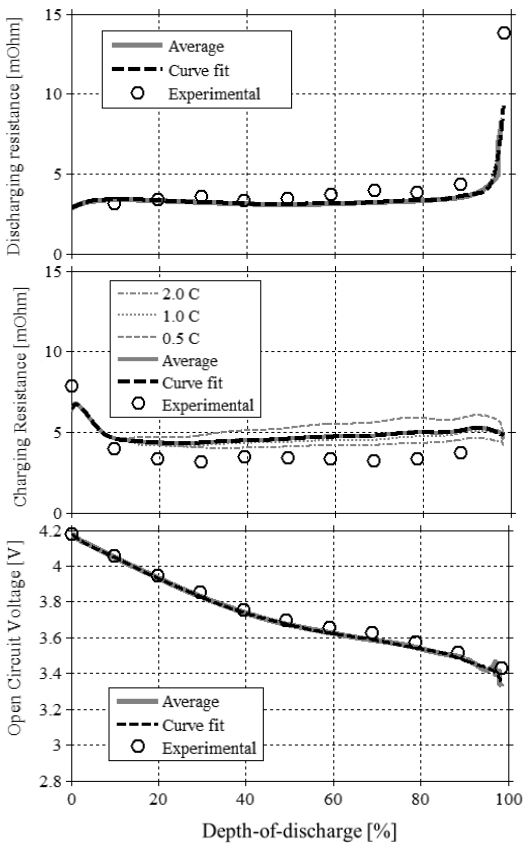


Fig. 14: ECM III: Estimated inner resistances and OCV characteristic vs. experimental results from 1C-rate pulsed current tests.

## REFERENCES

[1] A. Jossen, "Fundamentas of battery dynamics," *Journal of Power Sources*, 154 (2006) 530–538.

[2] R. Spotnitz, "Battery Modeling," *The Electrochemical Society Interface*, pp. 39-42, Winter 2005.

[3] R. Rao, S. Vrudhula, D. N. Rakhmatov, "Battery Modeling for Energy-Aware System Design," *IEEE Computer*, vol. 36, issue 12, pages 77-87, December 2003, ISSN: 0018-9162.

[4] Chen M. and Rincon-Mora, G., "Accurate electrical battery model capable of predicting runtime and I-V performance," *IEEE Trans. Ener. Conv.* 21, 2, 504-511, 2006.

[5] D. N. Rakhmatov, "Battery voltage modeling for portable systems," *Journal ACM Transactions on Design Automation of Electronic Systems (TODAES)*, vol. 14, issue 2, ISSN: 1084-4309, March 2009.

[6] J. Kowal, J.Bernhard Gerschler, C. Schäper, T. Schoenen, D.U. Sauer, "Efficient battery models for the design of EV drive trains," 14th International Power Electronics and Motion Control Conference, EPE-PEMC 2010.

[7] O. Tremblay, L. A. Dessaint, "Experimental Validation of a Battery Dynamic Model for EV Applications," World Electric Vehicle Journal vol. 3, ISSN 2032-6653, 2009.

[8] W. Peukert, "Über die Abhängigkeit der Kapazität von der Entladestromstärke bei Bleiakkumulatoren," *Elektrotechnische Zeitschrift 20*, 1897.

[9] D. Doerffel, S. A. Sharkh, "A critical review of using the Peukert equation for determining the remaining capacity of lead-acid and lithium-ion batteries," *Journal of Power Sources*, vol. 155, issue 2, pp. 395-400, April 2006.

[10] L. Gao, S. Liu, R. A. Dougal, "Dynamic Lithium-Ion Battery Model for System Simulation," *IEEE Transactions on Components and Packaging Technologies*, vol. 25, no. 3, September 2002.